Investigation on initial oxidation kinetics of Al, Ni, and Hf metal film surfaces

Shigeng Song* **and Frank Placido**

Thin Film Centre, University of the West of Scotland, Paisley, Scotland PA1 2BE, England

**E-mail: shigeng.song@uws.ac.uk*

Received October 27, 2009

High precision, single-wavelength optical monitoring of reflectance was shown to be useful in the study of initial oxidation of very thin metal films by low pressure oxygen at room temperature. Thin films of Al, Ni, and Hf metal were sputter-deposited on silicon substrates and their subsequent oxidations were observed at low oxygen partial pressure using a temperature-stabilised laser diode reflectometer. Based on the derived properties of the appropriate metal and oxide films, optical monitoring data were fitted as a multilayer stack comprised of oxide/metal/SiO_2/Si. The fitting results show that the exposure to oxygen at a partial pressure of 0.04 Pa forms a certain finite thickness of oxide film on the metal surface. A range of kinetic models such as Deal-Grove, Massoud, and Cabrera-Mott are commonly used to describe the surface oxidation process. However, these models cannot be applied to the initial stage of oxidation, which occurs when a pure metal surface is exposed to oxygen as measured here. Instead, simple chemical reaction kinetics is used to model the time-dependent experimental results of the early stages of oxidation, thus we obtain the equation $d(t) = d_o[1-\exp(-t/\tau)]$ and $d(t) = d_o[1-1/(1+t/\tau)]$ for the gas environments of this investigation.

OCIS codes: 240.0240, 240.0310, 240.6648.

doi: 10.3788/COL201008S1.0087.

An oxide layer forms rapidly when a fresh metal surface is exposed to an oxygen-including atmosphere. At atmospheric pressure and room temperature, the layer is usually self-limiting, resulting in a so-called native-oxide layer with a thickness of a few nanometers. For example, in Banerjee's report[1], a silicon wafer had a native oxide layer of around 2 nm, while according to the investigation in Ref. [2] on the initial oxidation of Fe-nanoparticles, the typical thickness of the native oxide layer was said to be 2−3 nm.

The thickness of oxide formed on thin metal films is of interest for a number of applications. This is particularly so for metallisation layers used in the manufacture of backplanes for plastic electronics where two or more very thin layers of metal may be necessary to provide both adhesion to the polymer substrate and sufficiently low sheet resistance (e.g., Ti/Au, Ni/Au, Cr/Au, etc.). Even when no oxygen is deliberately introduced into the vacuum chamber, low levels may still be available to the metal films due to residual water vapour outgassing from the polymer substrate or the chamber walls. The degree and rate of oxidation of the less noble, adhesion-promoting layers at the typical oxygen pressures encountered in vacuum chambers are of great importance in determining the performance and lifetime of devices and are not easily measured after deposition is complete. In the course of researching alternative metallisation layers, we investigated the first stage of oxidation of several metals at low oxygen partial pressures and presented some initial results. Precise in-situ measurements of reflectance during the deposition and oxidation of thin metal films of Al, Ni, and Hf on silicon substrates were used to measure reliably extremely thin oxide films formed in very low oxygen partial pressures.

A range of kinetic models such as the Deal-Grove[3], Massoud[4], and Cabrera-Mott (CM) models[5,6] have been used to describe the surface oxidation of metals, but these are limited to subsequent thermal processes and are not valid for the initial oxidation, which occurs when a fresh metal surface is exposed to oxygen. Zhdanov *et al.* modified the CM model for the oxidation of nm-sized metal particles[7]. However, no clear result has been demonstrated to prove that the modified model agrees with the experiment. Lopez-Beltran *et al.* investigated the oxidation of nickel thin films, showing that the experimental data followed a parabolic equation[8]. In the absence of suitable models, simple chemical reaction kinetics was used here to model the experimental results of the time dependence of the very early stages of oxidation.

The in-situ investigation of surface oxidation of metal films was carried out in a microwave plasma-assisted pulsed-DC sputtering system described in the Refs. [9,10]. Appropriate dielectric functions of the metal films and fully oxidised films were known from the previous experiments using this equipment.

This system, equipped with a single wavelength optical monitoring system, is shown in Fig. 1. A temperature-stabilised laser diode operating at a wavelength of 670 nm provided a large and very stable signal to noise in reflectance mode. The laser entered the chamber through a window that we coated on both sides with an anti-reflection coating for 670 nm. Two metal targets, which are mounted on the left and right hand sides of the chamber, were available for deposition. The microwave plasma applicator was at the top position. The optical monitoring system was mounted at the 45° position on the right hand side. Substrates were mounted on a rotating drum. During film deposition, substrates on the rotating drum passed through the deposition area, microwave plasma area, and optical monitoring area sequentially. The versatile microwave plasma is also used for substrate pre-cleaning with argon gas mixtures, activation of reactive gases, and post-deposition treatment.

1671-7694/2010/S10087-04 © 2010 Chinese Optics Letters

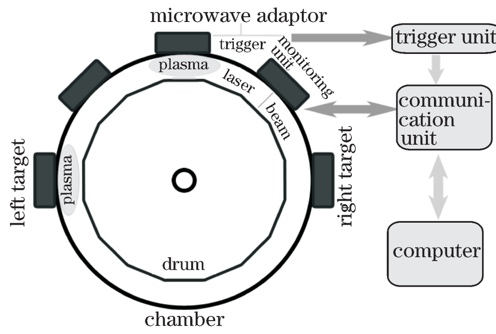

Fig. 1. Arrangement of the optical monitoring and deposition system.

Table 1. Refractive Index and Extinction Coefficient of Thin Ni, Al, and Hf Metal and Oxide Films

	Ni		Al		Hf	
	Metal	Oxide	Metal	Oxide	Metal	Oxide
n	2.3962	2.3465	1.7768	1.6453	3.6616	2.0926
k	3.9141	0.1234	7.5393	0	3.1098	0

To study oxidation by optical monitoring, metal films were deposited onto the silicon substrates, which were cleaned of organic residues using an argon microwave plasma step before deposition. The native oxide layer on the silicon substrates themselves was not affected by this step and was considered in later analysis. All metal films were then deposited without microwave plasma assistance and using 190 sccm of argon gas only. Immediately after deposition of the fresh metal films, 30 sccm of oxygen gas was introduced into the chamber to observe the initial oxidation of the metal film under the argon/oxygen environment. This equates to a partial pressure of 0.04 Pa in the chamber. Note that the future work will investigate how oxidation depends on partial pressure. The in-situ reflectance was recorded at normal incidence once per second as the drum rotates at 60 rpm.

A sharp decrease in the reflectance of the fresh metal films was observed when oxygen gas was first introduced into the vacuum chamber. However, there was no change in the reflectance of the silicon films when oxygen was introduced into the chamber prior to metal deposition. This confirms that the reduction in reflectance is due to the reactions on the metal film surface and not simply due to the presence of oxygen.

The values of n and k at 670 nm used for fitting the reflectance data are given in Table 1 for thin Ni, Al, and Hf metal and oxide films. These were obtained from previous measurements of sputtered films.

A silicon substrate was used for optical monitoring. Due to the excellent signal to noise ratio obtained with the laser reflectometer, the measured reflectance was also very sensitive to the presence of a native oxide layer on silicon. By fitting the data obtained before metal layer deposition, it was found that there was a 2 nm thick native oxide on the surface of the silicon substrate. The refractive index and extinction coefficient of Si and SiO_2 are well known. Combined with the refractive index and extinction coefficient of the metals and oxides from Section 3, we have almost all the parameters needed for the simulation and fitting of the optical monitor data (assuming refractive index homogeneity in the layers).

Here, we have an unusual modelling problem in that the oxide layer is formed from the already deposited metal, and thus the metal film thickness and the oxide film thickness at any given time are related. A metal film of thickness $d_{\rm m}$ will lead to an oxide layer of thickness $d_{\rm o}$, wherein $d_{\rm o} \neq d_{\rm m}$ because of the density differences between the metal and the oxide. The last piece of information we need is a thickness correction factor, $f = d_{\rm o}/d_{\rm m}$. The number of metal atoms per unit area in a metal and oxide film can be obtained from

$$N_{\rm metal} = \frac{D_{\rm m} \times S \times d_{\rm m}}{A_{\rm m}} \times N_0, \quad (1)$$

$$N_{\rm oxide} = N_{\rm m} \times \frac{D_{\rm o} \times S \times d_{\rm o}}{M_{\rm o}} \times N_0, \quad (2)$$

where $D_{\rm m}$ and $D_{\rm o}$ are the densities, $d_{\rm m}$ and $d_{\rm o}$ are the thicknesses of the metal and oxide layer, respectively, $A_{\rm m}$ is the metal atomic weight, $M_{\rm o}$ is the oxide molecule weight, S is a unit area, $N_{\rm m}$ is the metal atom number in one oxide molecule, and N_0 is Avogadro's number. Here, $N_{\rm m}$ is 1, 2, and 1 for NiO, Al_2O_3, and HfO_2, respectively.

The number of metal atoms per unit area must remain the same before and after oxidation. Thus, we have $N_{\rm metal} = N_{\rm oxide}$, and the required thickness factor is

$$f = \frac{d_{\rm o}}{d_{\rm m}} = \frac{D_{\rm m} \times M_{\rm o}}{D_{\rm o} \times A_{\rm m} \times N_{\rm m}}. \quad (3)$$

Finally, the thickness correction factors are obtained as 1.66, 1.28, and 1.48 for Ni, Al, and Hf, respectively.

The measured reflectance during Ni, Al, and Hf film deposition and oxygen exposure is shown in Fig. 2. By fitting the reflectance data, we obtained the metal layer thicknesses and oxide layer thicknesses as a function of time. The layer stack used for fitting the growing metal layers was metal-layer/2-nm-SiO_2/Si. For the oxidation stage, a layer stack of oxide-layer/metal-layer/2-nm-SiO_2/Si was used. If the final deposited thickness of the metal film is $d_{\rm final}$, and the remaining metal thickness at a given time is d, then the oxide thickness is constrained to be $f(d_{\rm final}\text{-}d)$, where f is the thickness correction factor derived in Eq. (3) above. A program

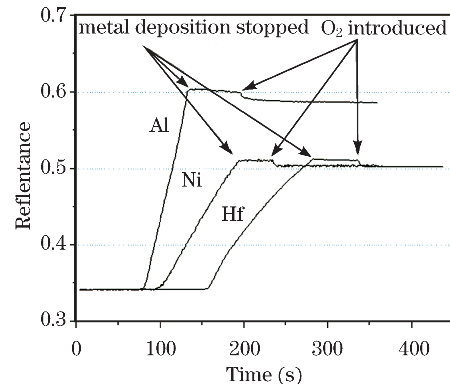

Fig. 2. Reflectance versus time for Ni, Al, and Hf deposition and surface oxidation.

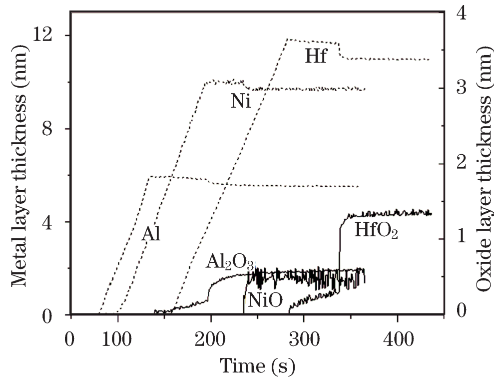

Fig. 3. Metal and oxide thickness versus time for Ni, Al, and Hf deposition and surface oxidation.

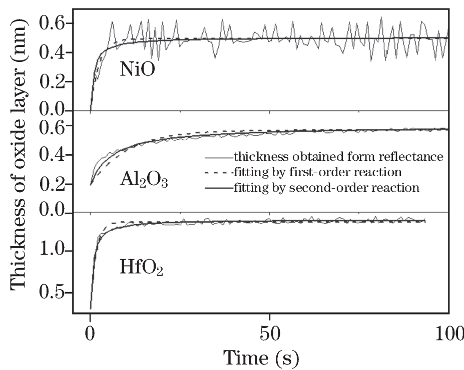

Fig. 4. Fittings for oxide layer thickness against time by chemical reaction kinetics.

Table 2. Fitting Parameters for the Initial Oxidation of Ni, Al, and Hf Surface

	First-order Reaction			Second-order Reaction		
	d_{01}(nm)	d_{02} (nm)	τ (s)	d_{01}(nm)	d_{02} (nm)	τ (s)
Ni	0	0.49	2.24	0	0.50	0.89
Al	0.19	0.38	9.87	0.19	0.41	5.82
Hf	0.31	1.02	1.47	0.31	1.05	0.73

for fitting the reflectance data was written in Mathcad. The calculated thicknesses of the remaining metal and growing oxide layer against time are shown in Fig. 3.

On the Al and Hf surfaces we found that an oxide layer began to form at a growth rate of 0.034 Å/s on Al and 0.058 Å/s on Hf even before the introduction of oxygen, but no such effect was observed for the Ni film. This oxidation is presumably due to the small residual oxygen partial pressure in the chamber and the affinity of Al and Hf for oxygen. Thus, there was already an oxide layer of 0.19 nm on Al surface and 0.31 nm on Hf surface at the time when oxygen was deliberately introduced into the chamber. At this point, the reflectance of all samples showed a sharp downwards jump.

The fitting results show that the oxide layer thicknesses all stabilise in a very short time after the introduction of oxygen. The finite thicknesses are 0.52, 0.6, and 1.35 nm for NiO, Al_2O_3, and HfO_2, respectively, under a 4.5 mTorr chamber pressure with Ar gas flow of 190 sccm and O_2 partial pressure of 0.04 Pa.

Initial surface oxidation is a complex process. Oxygen molecules must collide with the surface and become absorbed as molecules or atoms. The trapped oxygen may diffuse or dissolve in a thin surface layer. Oxide nucleates form in this thin layer at favourable sites. The nucleates then grow to form a complete thin oxide film[11]. The surface oxide layer usually reaches a finite thickness of a few nanometers at room temperature and atmospheric pressure, being limited by the diffusion of oxygen through the oxide layer to reach unreacted metal. Surface reconstruction can also occur during metal surface oxidation, and the metal surface morphology and defects are important factors for surface oxidation as well. Yang *et al.*[12] developed a description of the initial oxidation process by using the heteroepitaxial concept of a "zone of oxygen capture". The coverage of oxide nucleation on film surface can be fitted very well by the following equation[12]

$$N = 1 - \exp\left(-kL_d^2 t\right), \tag{4}$$

where N is the number density of nuclei, and L_d^2 is the area of the zone of oxygen capture.

As it describes the oxide nuclei coverage, it is difficult to use this equation to analyse how the thickness of the initial oxide layer changes with time. Here, we will use a generalized approach of chemical reaction kinetics. We assume that only the metal surface layer of a certain thickness will be oxidised, as initial oxidation stops at about a few nanometers. The oxidation rate depends on the concentration of the metal element on this surface layer. By using integrated rate laws[13], we obtain the following equations.

For a first-order reaction

$$d(t) = d_{02}\left[1 - \exp\left(-\frac{t}{\tau}\right)\right] + d_{01}. \tag{5}$$

For a second-order reaction

$$d(t) = d_{02}\left[1 - \frac{1}{1 + t/\tau}\right] + d_{01}, \tag{6}$$

where $(d_{01} + d_{02})$ is the final thickness of the native oxide layer when t intends to infinity.

Let d_{01} be equal to zero. Rewriting Eq. (5), we have

$$\frac{d(t)}{d_{02}} = 1 - \exp\left(-\frac{t}{\tau}\right). \tag{7}$$

It is clear that Eq. (7) has a similar format with Eq. (4). The reason is that Eq. (4) is obtained with the assumption that the probability of an oxide nucleation event is proportional to the fraction of the available surface area outside these zones of capture, which is the idea of chemical reaction kinetics.

Using Eqs. (5) and (6), the thickness of the oxide layer against time is fitted (Fig. 4). The first-order equation fits the Ni surface oxidation slightly better than the second-order equation does. However, the fittings using the second-order equation for Al and Hf surface oxidation are far better than those using the first-order equation.

The fitting parameters for the initial oxidation of Ni, Al, and Hf surface are shown in Table 2. The d_{01} are not zero for Al and Hf because there was already a thin

oxide layer before oxygen was introduced, although no oxide layer was found at this stage for Ni. According to the reaction time constant τ, the reaction speed of Al is much slower than others. The final initial oxide thicknesses are about 0.50, 0.60, and 1.36 nm for Ni, Al, and Hf, respectively.

In conclusion, initial oxidation of Ni, Al, and Hf metal film surfaces at a partial pressure of 0.04 Pa was studied in our sputtering system (MicroDyn 40000) using an in-situ single wavelength monitoring system. This laser-based system was demonstrated to be suitable for measuring changes in reflectance due to the extremely thin layers of metal and oxide.

Using the refractive index and extinction coefficient of these metals and oxides previously obtained from the sputtering system, the optical monitor data for surface oxidation were fitted using an appropriate layer stack and optical models.

Therefore, kinetic equations of the initial stages of oxidation were developed using chemical reaction kinetics. The first-order equation fits Ni surface oxidation slightly better than the second-order equation does. However, fits to the second-order equation to Al and Hf surface oxidation are far better than those to the first-order equation. According to the derived reaction time constants τ, the reaction rate of Al is much slower than that of Hf and Ni. The final initial oxide thicknesses are about 0.50, 0.60, and 1.36 nm for Ni, Al, and Hf, respectively.

This work was supported by EPSRC and DTI (now TSB) under Grant No. DT/E010830/1.

References

1. I. Banerjee, J. Electrochem. Soc. **140,** 501 (1993).
2. C. M. Wang, D. R. Baer, J. E. Amonette, M. H. Engelhard, J. J. Antony, and Y. Qiang, Micorsc. Microanal **12,** 546 (2006).
3. S. A. Campbell, *The Sctence and Engineering of Microelectronic Fabrication* (Oxford University Press, London, 1996).
4. H. Z. Massoud, J. D. Plummer, and E. A. Irene, J. Electrochem. Soc. **132,** 2693 (1985).
5. N. Cabrera and N. Mott, Rept. Prog. Phys. **12,** 163 (1984).
6. V. P. Parkhuttik, J. Phys. D: Appl. Phys **25,** 256 (1992).
7. V. P. Zhdanov and B Kasemo, Chem. Phys. Lett. **452,** 285 (2008).
8. A. M. Lopez-Beltran and A. Mendoza-Galvan, Thin Solid Film **503,** 40 (2006).
9. S. Moh and F. Placido, in *Proceedings of 47th Annual Technical Conference Proceedings of the Society of Vacuum Coaters* 443 (2004).
10. F. Placido and A. Voronov, in *Proceedings of the 45th Annual Technical Conference of the Society of Vacuum Coaters* 266 (2002).
11. J. R. Davis, *Heat-resistant materials* (ASM International, New York, 1997)
12. J. C. Yang, M. D. Bharadwaj, G. Zhou, and L. Tropia, Microsc. Microanal. **7,** 486 (2001).
13. D. N. Blauch, "Chemical Kinetics, Integrated Rate Laws" http:// www.chm. davidson.edu/ vce/kinetics /IntegratedRateLaws.html (December 1, 2009)